Cement and Concrete Research 39 (2009) 814–824

Contents lists available at ScienceDirect

Cement and Concrete Research

journal homepage: http://ees.elsevier.com/CEMCON/default.asp

Evaluation of chloride penetration in high performance concrete using neural network algorithm and micro pore structure

Ha-Won Song [a,*], Seung-Jun Kwon [a,b]

[a] Department of Civil Engineering, Yonsei university, Seoul, 120-749, Republic of Korea
[b] Department of Civil and Environmental Engineering, University of California, Irvine, United States

ARTICLE INFO

Article history:
Received 11 December 2007
Accepted 28 May 2009

Keywords:
Chloride attack
Chloride penetration behavior
Diffusion coefficient
Neural network
High performance concrete (HPC)

ABSTRACT

Chloride attack is one of the major causes of deterioration of reinforced concrete structures. In order to evaluate the chloride behavior in concrete, a reasonable prediction for the diffusion coefficient of chloride ion, which governs mechanism of chloride diffusion inside concrete, is basically required. However, it is difficult to obtain chloride diffusion coefficients from experiments due to time and cost limitations.
In this study, a numerical technique for chloride diffusion in high performance concrete (HPC) using a neural network algorithm is proposed. In order to collect comparative data on diffusion coefficients in concrete with various mineral admixtures such as ground granulated blast-furnace slag (GGBFS), fly ash (FA), and silica fume (SF), a series of electrically driven chloride penetration tests was performed. Seven material components in various mix designs and duration time are selected as neurons in a back-propagation algorithm, and associated learning of the neural network is carried out. An evaluation technique for chloride behavior in HPC using the obtained diffusion coefficients from the neural network algorithm is developed based on, so-called, Multi-Component Hydration Heat Model (MCHHM) and Micro Pore Structure Formation Model (MPSFM). The applicability of the developed technique is verified by comparing the analytical simulation results and the experimental results obtained in this study. Furthermore, this proposed technique using the neural network algorithm and micro modeling is applied to available experimental data for verification of its applicability.

1. Introduction

Even concrete is considered as an economical and durable construction material, concrete structures show degradation of durability as well as structural performance in severe environmental condition. Quantitative data on chloride penetration is essential to predict the residual service life of concrete structures due to chloride attack, because chloride ion directly affects degradation of durability performance and further the structural safety of concrete structures due to chloride induced reinforcement corrosion. The research field on evaluation of chloride diffusion in concrete is growing with consideration for diffusion, permeation [1] and binding capacity of chloride ions [2,3]. Recently, numerical techniques covering chloride diffusion in partially saturated condition [4], chloride behavior in concrete with early-age cracking [5], and micro structures formation modeling in high performance concrete [6,7] are proposed based on behavior in early-age concrete considering hydration and micro pore structure. Among parameters such as diffusion coefficient, humidity, temperature, and mixture proportions, the diffusion coefficient of chloride ion is the most significant parameter to be derived for prediction of service life or residual life of concrete structures. Several simple equations for apparent diffusion coefficient obtained from regression analysis with water to cement ratio (W/C) or replacement ratio of mineral admixtures are generally used for the prediction of service life in the Standard Specification [8,9] and conventional analysis tools [10]. However, they have a limited applicability, e.g., which cannot consider various characteristics in mix design. Recently, some researches on neural network in data processing are introduced in the field of durability and they are very efficient compared with simple regression method obtained from experimental data. In area of research on concrete, a neural network technique is mainly applied to mixture design [11–14], strength evaluation [15,16], and reaction of hydration [17,18]. In this study, a neural network technique, which is mainly utilized in mixture design and strength evaluation, is applied for estimation of chloride diffusion coefficient. The estimation of diffusion coefficient through neural network considering various components in mixture design and the development of analysis technique with the estimated diffusion coefficient are meaningful for quantitative evaluation for chloride behavior in concrete.

In this paper, electrically driven chloride penetration tests for diffusion coefficient are performed for the concretes with various

* Corresponding author. Tel.: +82 2 2123 2806.
E-mail address: song@yonsei.ac.kr (H.-W. Song).

0008-8846/$ – see front matter
doi:10.1016/j.cemconres.2009.05.013

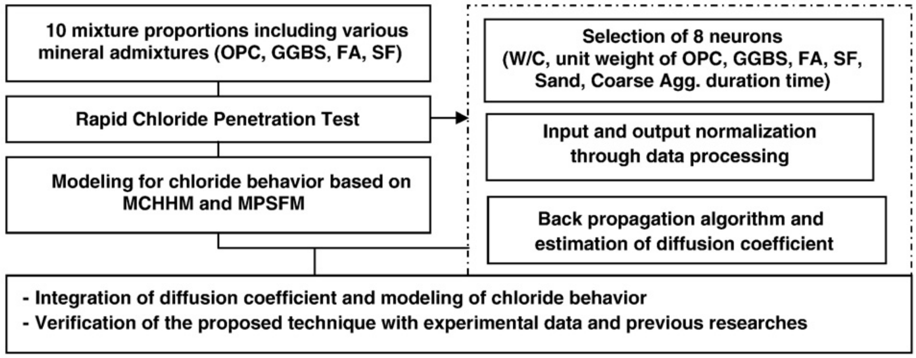

Fig. 1. Flowchart of this study.

parameters such as W/C ratios (37%, 42% and 47%), mineral admixtures like ground granulated blast-furnace slag (GGBS), fly ash (FA), silica fume (SF) with different replacement ratios. Secondly, 120 diffusion coefficients obtained from experiment are analyzed through neural network algorithm and diffusion coefficients are also estimated. Then, the estimated coefficients are applied to numerical modeling for chloride penetration based on Multi-Component Hydration Heat Model(MCHHM) and Micro Pore Structure Formation Model(MPSFM) [4,7,18]. Finally, the numerical simulation results of chloride diffusion from the proposed model with neural networks are compared with experimental results. A reasonable agreement with obtained results confirms the applicability of the proposed model. The flowchart of this study is shown in Fig. 1.

2. Estimation from neural network algorithm

2.1. Background of neural network

An overview study on neural network algorithms is provided by McCulloch and Pitt [19]. A neuron as a unit with process of stimulus and reaction is generalized in this system. The training for learning a set of data is performed with weight (connection strength), transfer function, and biases. The error between calculated results and expected results is decreased with increasing epochs and training for learning is finished within a target convergence.

In this study, a back-propagation algorithm is used for the neural network. Fig. 2 shows an outline of a simple neural network architecture [20].

In this network, each element of input value is connected to each neuron input through the weight matrix. Neurons (N_j) and activated values (H_j) in the hidden layer are formulated as Eqs. (1) and (2).

$$N_j = \sum W_{ji} I_i \tag{1}$$

$$H_j = f\left(N_j + B_j\right) \tag{2}$$

where I_i is input value, W_{ji} is the weight or the connection strength, f is the transfer function, B_j is bias. Activated value (O_k) can be written as Eq. (3).

$$O_k = f\left(\sum W_{kj} H_j + B_k\right) \tag{3}$$

In the back-propagation algorithm, error (E) is formulated as Eq. (4) concerning target value (T_k).

$$E = \frac{1}{2}\left(\sum_{k=1} O_k - T_k\right)^2 \tag{4}$$

To minimize this error, weights or connection strength are modified backward from neurons in output layer and the weights are modified as per Eqs. (5) and (6), respectively.

$$\Delta W_{kj} = \eta \delta_k H_j,\ \Delta B_k = \eta \delta_k,\ \delta_k = (T_k - O_k) f'(N_k) \tag{5}$$

$$\Delta W_{ji} = \eta \delta_j H_i,\ \Delta B_j = \eta \delta_j,\ \delta_j = \left(W_{kj}\delta_k\right) f'\left(N_j\right) \tag{6}$$

where δ_j and δ_k are gradients of the total error, and η is the learning rate.

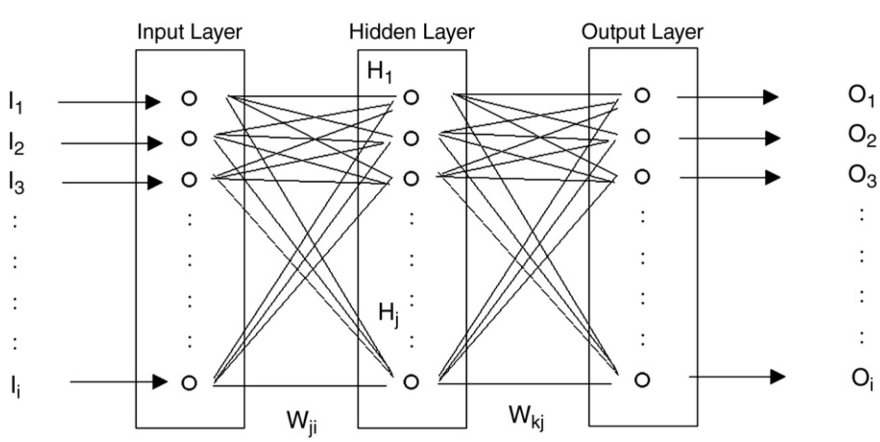

Fig. 2. Outline of simple neural network architecture [20].

Table 1
Condition of accelerated test.

Conditions		Levels	Cell
Electrolyte	Cathode	0.5 Mole NaCl	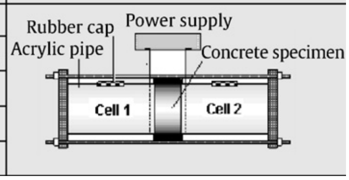
	Anode	Saturated $Ca(OH)_2$	
Applied voltage (V)		30	
Thickness (mm)		50	
Duration time (hour)		8	

After the finishing modification, the neural network algorithm repeats the calculation and modification process until error decreases within the target convergence. Each input and output value has boundary limits from 0.0 to 1.0 so it is necessary to perform data processing. Data processing for input and output is described as Eq. (7).

$$P_n = \frac{P_{\text{acutal}} - P_{\min}}{P_{\max} - P_{\min}} \tag{7}$$

where P_n is input value for training of learning, P_{acutal} is actual input data, $P_{\max}$ and $P_{\min}$ are maximum and minimum value of a set of input data.

2.2. Estimation for chloride diffusion coefficient through rapid chloride penetration test

2.2.1. Experiment program for acquisition of diffusion coefficient

It is difficult to assume the reasonable diffusion coefficient in concrete with various mineral admixtures without conducting experiment. The diffusion cell and experimental set up is provided in ASTM C 1202 [21] and the calculation of the diffusion coefficient is performed by an electrical method (non-steady state migration diffusion coefficient) proposed by previous researches [22,23]. Silver nitrate solution (0.1 N, $AgNO_3$) is used as an indicator [24]. The diffusion coefficient in non-steady state conditions is calculated through Eqs. (8) and (9).

$$D_{\text{cpd}} = \frac{RTL}{zFU} \cdot \frac{x_{\text{d}} - \alpha\sqrt{x_{\text{d}}}}{t} \tag{8}$$

$$\alpha = 2\sqrt{\frac{RTL}{zFU}} \cdot erf^{-1}\left[1 - \frac{2C_{\text{d}}}{C_0}\right] \tag{9}$$

where D_{cpd} is diffusion coefficient in non-steady state condition from RCPT (m^2/s), R is universal gas constant (8.314 J/mol K), T is absolute temperature (K), L is thickness of specimen (m), z is ionic valence (=1.0), F is Faraday constant (=96,500 J/V mol), U is applied potential (V), t is test duration time (s), C_{d} is the chloride concentration at which the color changes when using a colorimetric method to measure x_{d} based on the reference [22,24], C_0 is chloride concentration in the upstream solution (mol/l), α is an experimental constant, erf^{-1} is the inverse function of the error function. According to the previous research [22], $erf^{-1}(1-(2C_{\text{d}}/C_0))$ is calculated as 0.764 and zFU/RTL is 23,600 (m^{-1}) in this study. The

Table 2
Chemical composition of cement and physical properties of mineral admixtures used.

Items	Chemical composition (mass %)							Physical properties	
Types	SiO_2	Al_2O_3	Fe_2O_3	CaO	MgO	SO_3	Ig. loss	Specific gravity (g/cm^3)	Blaine (cm^2/g)
NPC	21.96	5.27	3.44	63.41	2.13	1.96	0.79	3.16	3,214
GGBS	32.74	13.23	0.41	44.14	5.62	1.84	0.2	2.89	4,340
FA	55.66	27.76	7.04	2.70	1.14	0.49	4.3	2.19	3,621
SF	93.3	0.5	1.21	0.27	1.03	0.02	1.1	2.21	190,620

Table 3
Mixture proportions for the tests.

Code: names of mixture	W/B (%)	S/a (%)	Unit weight (kg/m^3)							% of binder used	
			W	Binding materials				S	G	Admixture	
				C	GGBS	FA	SF			SP	AE
NPC100-37	37	45	168	454	–	–	–	767	952	1.0	0.017
NPC100-42	42	45	168	400	–	–	–	787	976	0.9	0.015
NPC100-47	47	47	168	357	–	–	–	838	960	0.85	0.017
G30N70-37	37	45	168	318	136	–	–	762	946	0.8	0.018
G30N70-42	42	45	168	280	120	–	–	783	972	0.75	0.013
G30N70-47	47	47	168	250	107	–	–	835	956	0.65	0.015
G50N50-37	37	45	168	227	227	–	–	760	943	0.75	0.017
G50N50-42	42	45	168	200	200	–	–	780	969	0.7	0.0135
G50N50-47	47	47	168	178	179	–	–	832	953	0.6	0.015
F10N90-37	37	45	168	409	–	45	–	760	943	0.75	0.018
F10N90-42	42	45	168	360	–	40	–	780	969	0.9	0.021
F10N90-47	47	47	168	321	–	36	–	832	952	0.75	0.017
F20N80-37	37	45	168	363	–	91	–	752	934	0.75	0.018
F20N80-42	42	45	168	320	–	80	–	774	961	0.85	0.025
F20N80-47	47	47	168	286	–	71	–	826	946	0.7	0.017
F30N70-37	37	45	168	318	–	136	–	745	952	0.75	0.2
F30N70-42	42	45	168	280	–	120	–	768	953	0.75	0.015
F30N70-47	47	47	168	250	–	107	–	820	939	0.65	0.019
F10S05-37	37	45	168	386	–	45	23	756	938	1.0	0.023
F10S05-42	42	45	168	340	–	40	20	777	965	0.9	0.021
F10S05-47	47	47	168	303	–	36	18	829	950	0.9	0.021
F20S05-37	37	45	168	340	–	91	23	749	929	0.9	0.023
F20S05-42	42	45	168	300	–	80	20	771	957	0.85	0.025
F20S05-47	47	47	168	268	–	71	18	810	927	0.9	0.025
G30S05-37	37	45	168	295	136	–	23	759	942	0.75	0.015
G30S05-42	42	45	168	260	120	–	20	765	949	0.75	0.015
G30S05-47	47	47	168	232	107	–	18	832	952	0.8	0.015
G35F15-37	37	45	168	227	159	68	–	751	932	0.65	0.014
G35F15-42	42	45	168	200	140	60	–	773	959	0.65	0.014
G35F15-47	47	47	168	178	125	54	–	804	921	0.7	0.014

Table 4
Test results for chloride diffusion coefficient with different curing period.

Code: names of mixture	Diffusion coefficient $\times 10^{-11}$ (m^2/s)			
	28 days	91 days	180 days	270 days
NPC100-37	1.3	1.1	0.8	0.7
NPC100-42	1.5	1.4	1.1	0.94
NPC100-47	1.8	1.6	1.5	1.2
G30N70-37	0.93	0.71	0.67	0.43
G30N70-42	1.1	0.76	0.76	0.54
G30N70-47	1.2	0.84	0.80	0.64
G50N50-37	6.3	0.37	0.25	0.24
G50N50-42	0.86	0.53	0.47	0.32
G50N50-47	1.1	0.72	0.65	0.43
F10N90-37	1.4	0.91	0.77	0.63
F10N90-42	1.5	1.0	0.94	0.76
F10N90-47	1.7	1.2	1.1	1.0
F20N80-37	1.3	0.66	0.57	0.45
F20N80-42	1.6	1.0	0.69	0.58
F20N80-47	1.9	1.1	0.93	0.70
F30N70-37	1.3	0.72	0.50	0.47
F30N70-42	1.6	0.81	0.54	0.52
F30N70-47	2.2	0.95	0.74	0.62
F10S05-37	0.69	0.42	0.31	0.24
F10S05-42	0.78	0.54	0.41	0.33
F10S05-47	0.89	0.67	0.48	0.36
F20S05-37	0.60	0.41	0.35	0.29
F20S05-42	0.71	0.64	0.48	0.45
F20S05-47	0.88	0.73	0.64	0.61
G30S05-37	0.53	0.33	0.23	0.22
G30S05-42	0.58	0.41	0.28	0.25
G30S05-47	0.61	0.48	0.31	0.29
G35F15-37	0.50	0.38	0.31	0.27
G35F15-42	0.65	0.40	0.36	0.29
G35F15-47	0.88	0.54	0.45	0.43

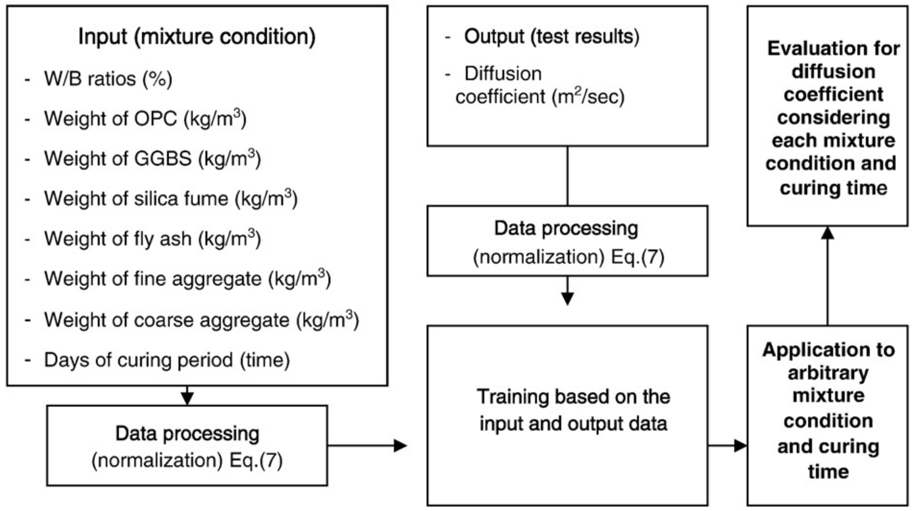

Fig. 3. Flow chart for application of neural network algorithm—input and output.

condition of the accelerated test, properties of cement compounds and mineral admixtures, and mixture proportions are summarized in Tables 1–3, respectively. In Table 1, the types of electrolyte are selected according to the previous work [23] and information on cement and aggregates are listed in Table 2.

In Table 3, NPC100-A denotes concrete with only OPC and W/C (A%) ratio. GANB-C denotes concrete with GGBFS A% replacement ratio, OPC B% replacement ratio, W/B (C%) ratio. In using fly ash, FANB-C denotes fly ash A% replacement ratio, OPC B% replacement ratio, W/B (C%) ratio and S means the replacement ratio of silica fume. In Table 4, the test results for diffusion coefficient with different curing period are listed, which are used for training the output values in neural network algorithm.

2.2.2. Estimation of diffusion coefficient with neural network algorithm

For using neural network with back-propagation, 8 input values are set up as neurons involving W/B ratio, unit weight of OPC, GGBS, fly ash, silica fume, sand, coarse aggregate, and duration time in submerged condition. Output value is determined as diffusion coefficient of chloride ion. In data processing for input values, $P_{\max}$ and $P_{\min}$ are assumed as 1000 and 0.0, respectively, and for output values, $P_{\max}$ and $P_{\min}$ are assumed as 20.0×10^{-12} (m^2/s) and 0.0 (m^2/s). In order to consider effective material components and decrease in diffusion coefficient with duration time, 7 components in mixture design and duration time (28 days, 91 days, 180 days, and 270 days) in submerged condition are selected as neurons. Tansig function is used as transfer function. Target epochs and mean square error are assumed as 1000 and 0.001, respectively. Flowchart for input/output value is shown in Fig. 3 and decrease in error with training is plotted in Fig. 4 showing the 519 epochs.

The comparison with the results of estimated diffusion coefficient and experimental data with 10% error bars is shown in Fig. 5. The lines are the simulated results (diffusion coefficient) through neural network algorithm. Generally, the estimated results represent the decrease in diffusion coefficient with increasing replacement ratio of GGBS, fly ash, silica fume, and duration time reasonably. The difference varies from 0.06% to 26% and average between experimental data and simulated data is evaluated to be 7.5% for 120 dataset. If the test results show better correlation, the difference between experimental and simulated data can be significantly reduced. The minimum chloride diffusion coefficient is measured in the case of high replacement ratio of GGBS with silica fume (OPC 65%, GGBS 30%, and silica fume 5%).

In FEM analysis, time-dependent effect on diffusion [25,26] is considered through regression analysis as Eq. (10). Each diffusion coefficient obtained from neural network and its respective time-parameter (m) is applied to FEM analysis.

$$D_{\mathrm{neural}}(t) = D_{\mathrm{neural28}} \cdot \left(\frac{t_{28}}{T_{\mathrm{duration}}}\right)^{m} \tag{10}$$

where $D_{\mathrm{neural}}(t)$ is time-dependent diffusion coefficient, D_{neural28} is estimated diffusion coefficient obtained from neural network at 28 days, t_{28} is reference time (=28 days), T_{duration} is duration time of chloride penetration. The time-parameter (m) is estimated to be 0.13–0.24 in concrete of OPC 100% and the higher values over 0.20 are estimated in concrete with mineral admixtures. The difference of time parameter mainly depends on increases in CSH gel and decreases in porosity through pozzolanic reaction, which is closely related with binder type of mixture.

3. Analysis for chloride penetration based on micro pore structure

3.1. Free and bound chloride content

The main route for transport of chloride ion is dependent on pore water which exists in the pores of concrete. So the relationship between

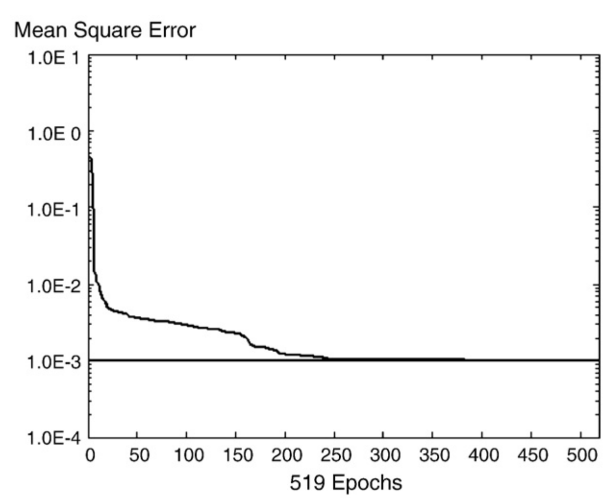

Fig. 4. Decrease in error with repeated training of learning.

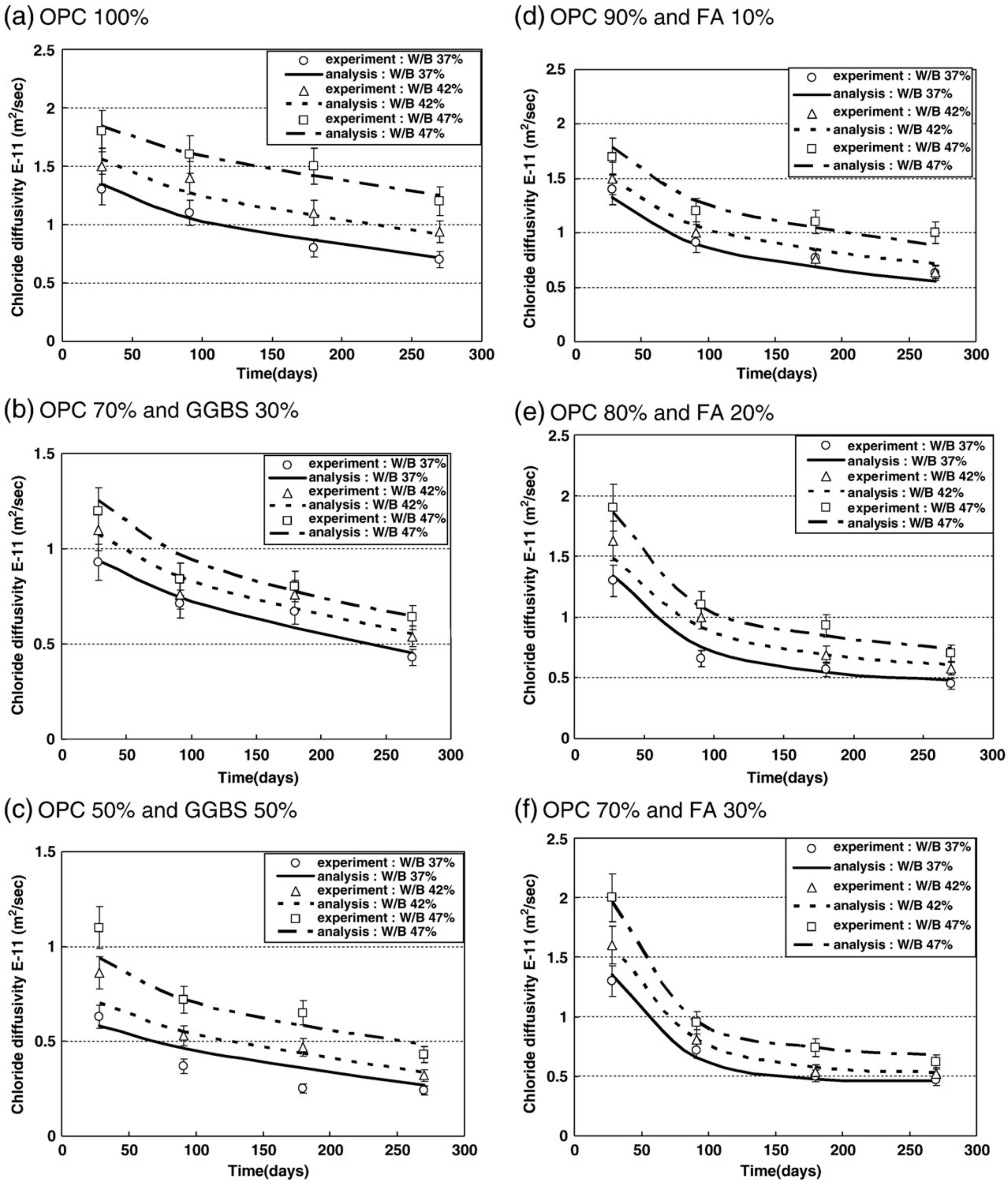

Fig. 5. Results of experiment and estimation.

chloride ion, C_{Cl} and free chloride content, C_{free} is determined by the pore water in concrete. In this paper, the free chloride content (kg/m^3) in unit volume of concrete can be obtained as Eq. (11).

$$C_{free} = C_{Cl} M_{Cl} \phi_{total} S V_{Sol} \tag{11}$$

where C_{Cl} (mol/l)is chloride ion concentration, M_{Cl} (kg/mol) is molar weight of chloride, ϕ_{total} is total porosity of concrete, S is saturation ratio, V_{Sol} is volume parameter of pore water in unit concrete volume (1000 l/m^3). Chloride ion in concrete can be divided into free chloride content which affects steel corrosion directly and bound chloride content which exists as chemically stable salts such as Friedel's salt. The bound chloride content is reported to be independent of W/C ratio or cement content but dependent on the type of binder, so long as not exposed to chemically unstable condition like carbonation [27,28]. In this study, a Freundlich isotherm [2] is used for the relationship between bound chloride content and chloride ion. For produced hydrates, porosity and system dynamics for describing their interactions including chloride ion transfer are based on Multi-Component Hydration Heat Model (MCHHM) and Micro Pore Structure Formation Model (MPSFM). These models can

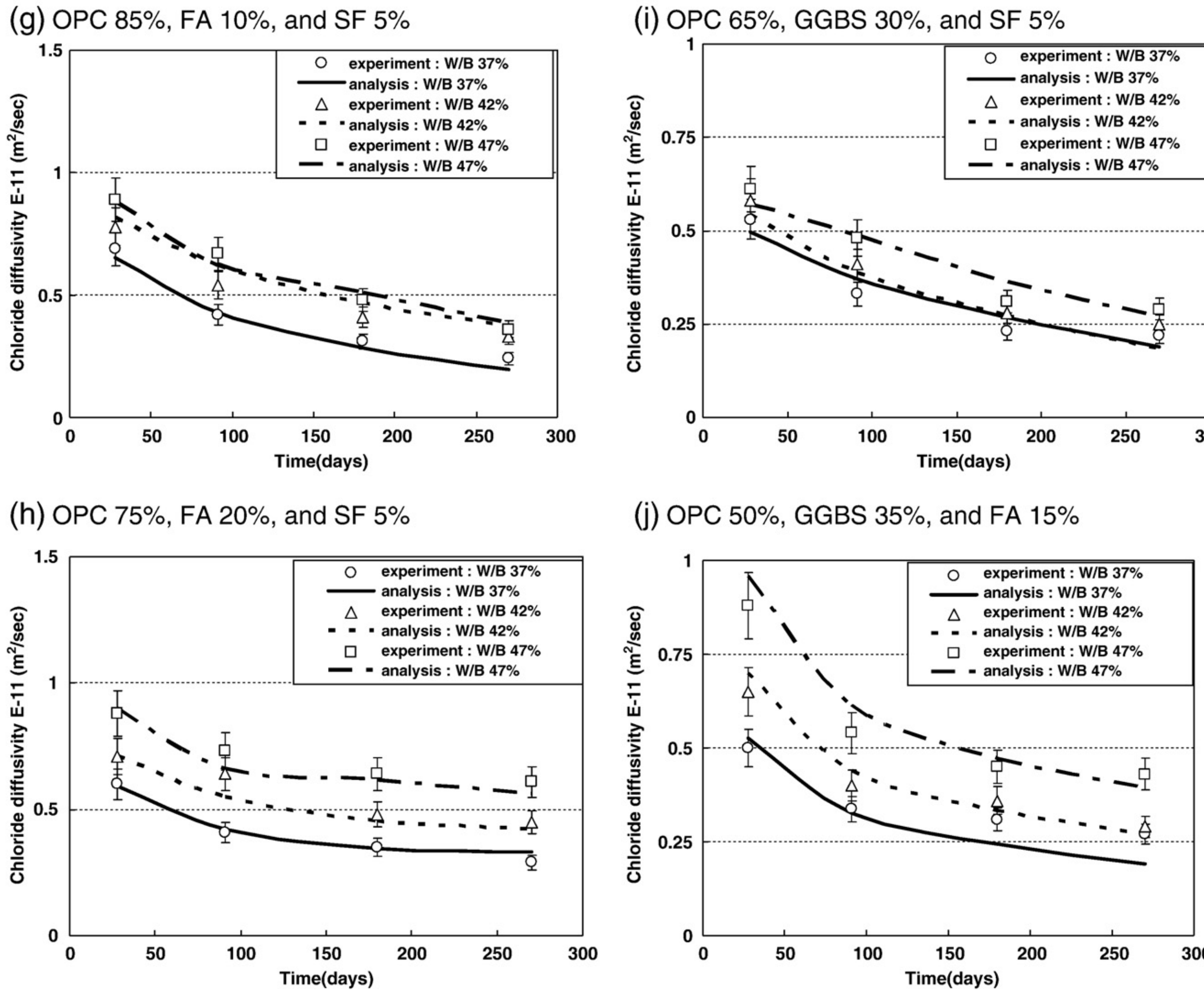

Fig. 5 (*continued*).

be found in previous reports [4,5,7,18,29–32]. Bound chloride content can be assumed as Eq. (12).

$$C_{\mathrm{bound}} = A \cdot \beta_{\mathrm{CSH}} \cdot W_{\mathrm{CONC}} \cdot C_{\mathrm{Cl}}^{B} = C(1-\phi_{\mathrm{Total}}) \cdot W_{\mathrm{CONC}} \cdot C_{\mathrm{Cl}}^{\mathrm{B}} \tag{12}$$

where A, B and C are material constants, β_{CSH} is weight ratio (weight of CSH gel/weight of concrete), W_{CONC} (kg/m^3) is weight of concrete, the constant, B is referred as previous work [2]. Silica fume (5%) effect on formation of CSH is not so significant that only decrease in porosity and diffusion coefficient is considered for simplicity of the analysis. Constants for FEM analysis of bound chloride content are shown in Table 5. The note for constants in Table 5 is adopted from previous work [2] and the other constants are assumed for the fitting the chloride profiles in this study.

3.2. FEM analysis for chloride penetration with neural network and system dynamics in early-age concrete

In order to simulate chloride behavior in concrete, porosity and saturation in early-age concrete should be provided in governing equation for mass and energy conservation in porous media given by Eq. (13)

$$\alpha_i \frac{\partial X_i}{\partial t} + divJ_i(X_i, \nabla X_i) - Q_i = 0 \tag{13}$$

where the first term is potential term, the second term is flux term and the last term is sink term of $[X_i]$ in Eq. (13). The details of $[X_i]$ and composition terms are explained in Table 6.

From Table 6, ρC is specific heat capacity, K_{H} is thermal conductivity, Q_{H} is heat generation rate, K_{l} and K_{v} are liquid and vapor conductivities, Q_{hyd} is combined water due to hydration. In this study, diffusion coefficient from neural network with time, $D_{\mathrm{neural}}(t)$, is used in governing equation.

Table 5
Constants for FEM analysis in this study.

Mixture type	$C_{\mathrm{bound}} = C(1-\phi_{\mathrm{Total}}) \cdot W_{\mathrm{CONC}} \cdot C_{\mathrm{Cl}}^{B}$	
	$C \times 10^3$	B
OPC 100%	3.57[a]	0.38[a]
Slag 30% replacement	3.82[a]	0.37[a]
Slag 50% replacement	5.87[a]	0.29[a]
Fly ash 10% replacement	3.78[b]	0.29[b]
Fly ash 20% replacement	3.78[b]	0.29[b]
Fly ash 30% replacement	3.78[b]	0.29[b]
Slag 35% + Fly ash 15% replacement	4.85[b]	0.33[b]

[a] Ref. [2].
[b] Assumed data.

Table 6
Terms used in governing equation for mass and energy conservation.

Variables [X_i]	Potential term	Flux term	Sink term
T [Temperature]	ρC [kcal/K m^3] -Constant	$-K_H \nabla T$ [kcal/m^2 s] -Constant	Q_H [kcal/m^3 s] -Multi-Component Hydration Heat Model of cement
P [Pore pressure]	$\phi\rho\frac{\partial S}{\partial P}$ [kg/Pa m^3] -Path dependent moisture isotherms	$-K_l+K_v\nabla P$ [kg/m^2 s] -Random geometry of pores and Knudsen vapor diffusion	$-Q_{hyd} - \frac{\partial(\rho S\phi)}{\partial t}$ [kg/m^3 s] -Water combined due to hydration; bulk porosity change effect
C_{Cl} [Chloride ion$^-$ concentration]	ϕS [mol l/mol m^3] -Path dependent chloride ion transport	$-D_{neural28}\left(\frac{t_{28}}{T_{duration}}\right)^m \nabla C_{Cl} + q_s C_{Cl}$ [mol/m^2 s] -Chloride diffusion obtained from neural network -Moisture diffusion and convection (q_s)	Q_{Cl}[mol/m^{3}s] -Bound chloride content along with Freundlich isotherm in unit time

Sink term (Q_{Cl}, bound chloride ion in unit time) in analysis of chloride penetration is considered as Eq. (14) [4,5].

$$Q_{Cl} = -\frac{C_{bound}^{n+1} - C_{bound}^{n}}{t_{n+1} - t_n} \tag{14}$$

A computational scheme of FEM analysis, based on framework of FEM program-DuCom developed by the University of Tokyo [4,17,18,31,32], for chloride penetration with neural network and system dynamics in early-age concrete is shown in Fig. 6.

4. Verification of test results for chloride penetration

Comparison with experimental and numerical results using diffusion coefficient from neural network is performed. Concrete specimens with various mineral admixtures as shown in Table 3 are prepared and they are cured in submerged condition for 28 days. After curing, they are submerged in 3.5% NaCl solution for 6 months. The specimens were coated with resin except for upside surface for 1-D intrusion of chloride ion. For evaluation of chloride profiles, acid-soluble chloride contents are measured based on the reference [33]. Total chloride content with 2.0 mm depth was obtained. Fig. 7 shows

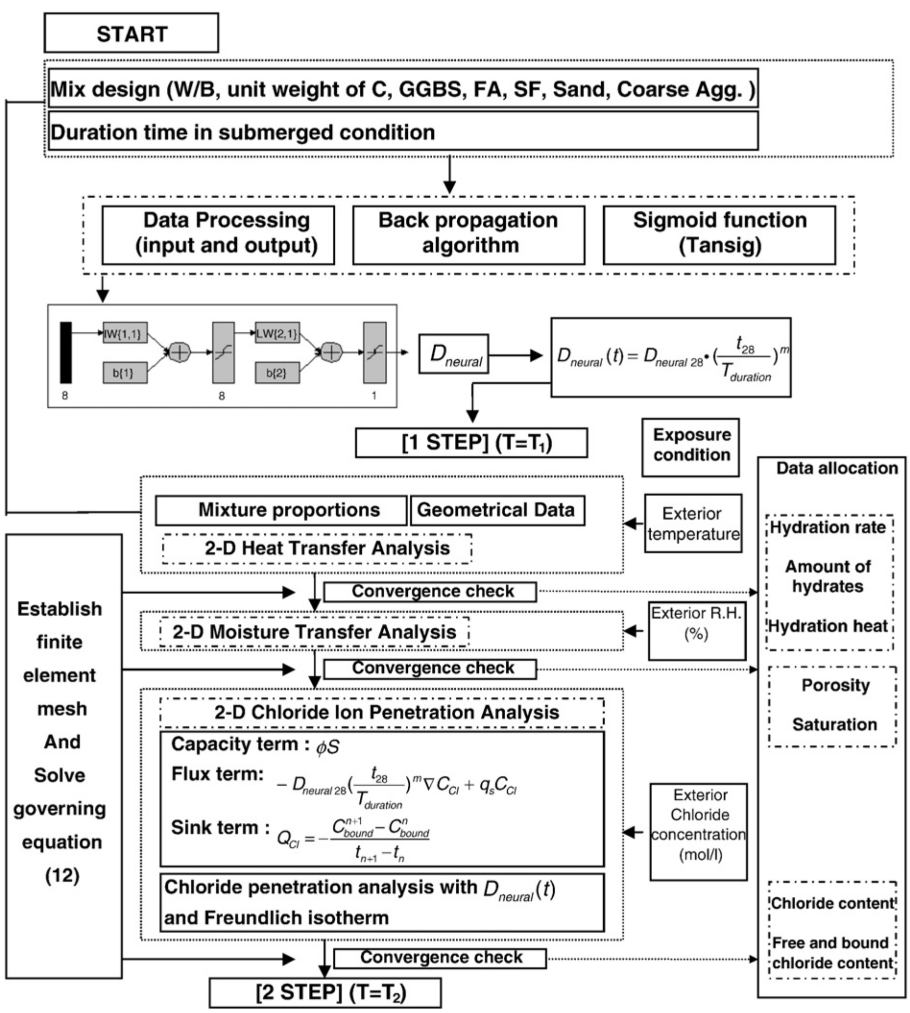

Fig. 6. Scheme of FEM analysis for chloride penetration with neural network and system dynamics.

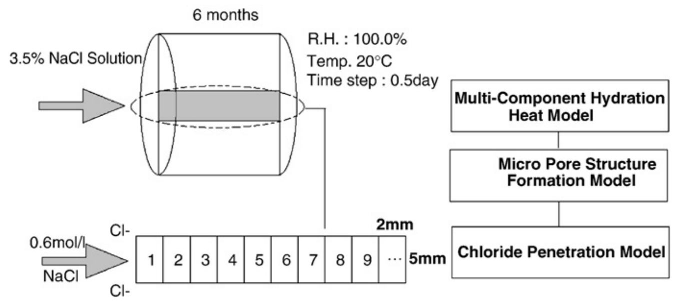

Fig. 7. Boundary condition and mesh generation for FEM analysis.

boundary condition and mesh generation for FEM analysis and Fig. 8 shows the results from experiment and FEM analysis with time-parameter (m) in Eq. (10).

Generally, the numerical results are in good agreement with experimental data. Some numerical data show more chloride intrusion than experimental data and it is expected that slightly higher diffusion coefficient is obtained in accelerated test and it causes the differences. The diffusion coefficient from this study is obtained from the electrically accelerated method and the data may be not enough to explain the pure diffusion of chloride ion in pore water which has various ions like potassium and calcic compound. However, these diffusion coefficients are obtained from convenient and relevant method [22,23]. For more idealized data-set, apparent coefficient from the specimens under long time submerged condition can be applied to this technique.

The calculated results of chloride behavior in concrete with same water to binder ratio are shown in Fig. 9. It is evaluated that chloride penetration in concrete with more mineral admixture is decreased in spite of higher surface chloride content. The reduced diffusion

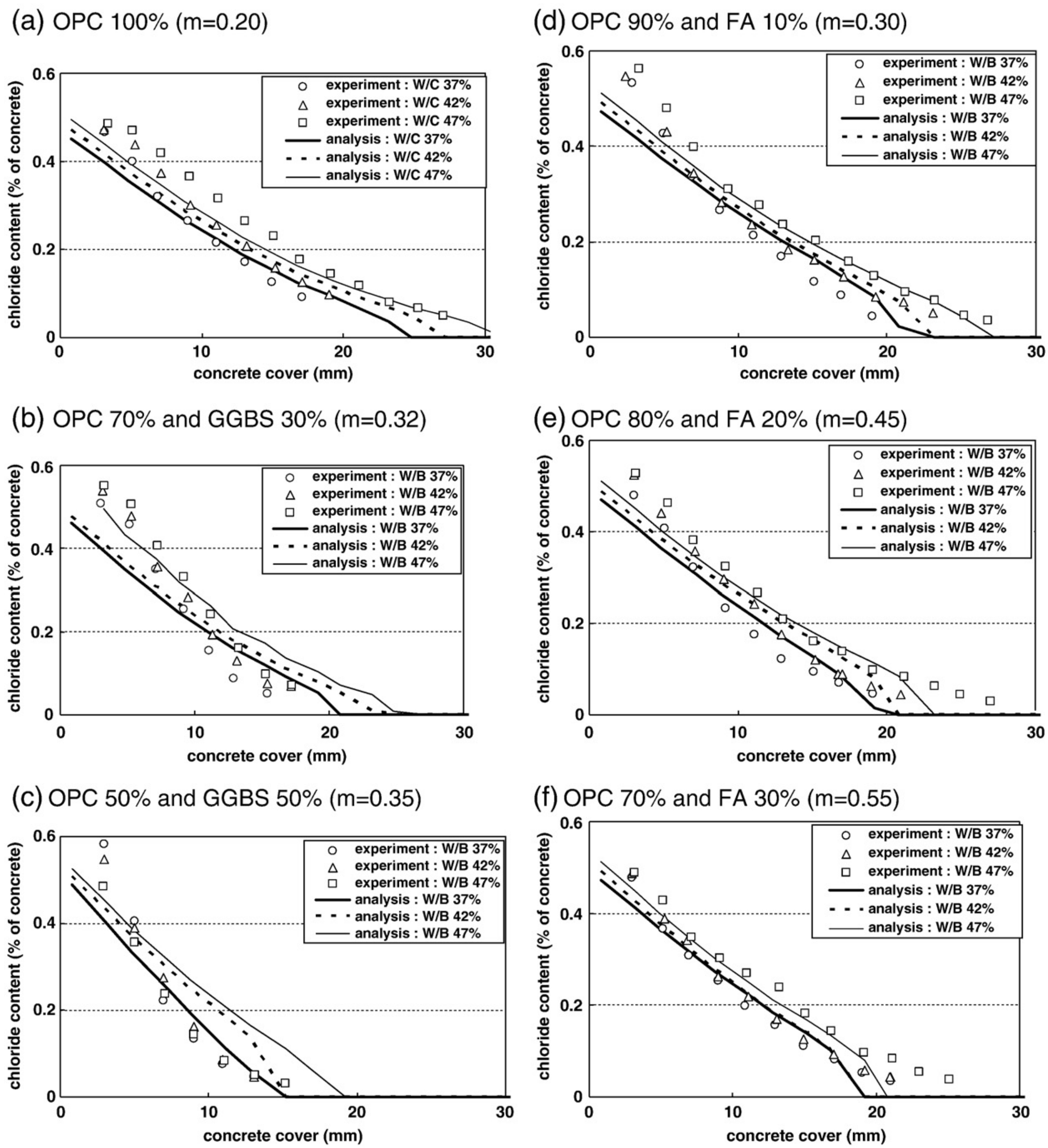

Fig. 8. Comparison with experimental and numerical results.

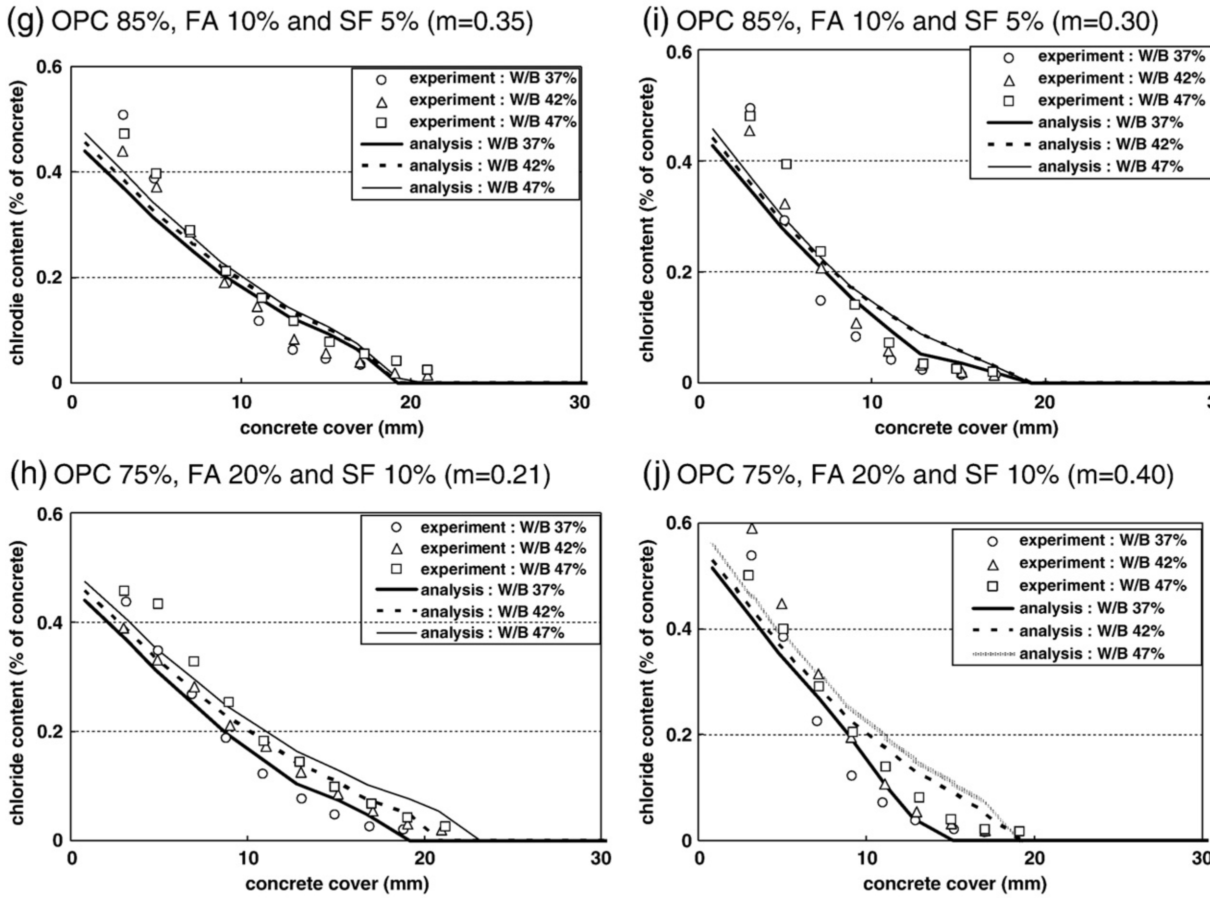

Fig. 8 (*continued*).

coefficient and magnified binding capacity due to mineral admixture make chloride-penetrated depth shorter and surface chloride contents higher, respectively.

This developed technique has the advantage of applicability to different mix design. Two mix designs where this technique is applied and estimated results of chloride diffusion coefficient are shown in Table 7. The comparisons of numerical and experimental results are shown in Figs. 10 and 11, where free chloride content in each case is simulated one. Reasonably this proposed technique is shown to predict the chloride behavior without experimentally obtained diffusion coefficient. The constants for binding capacity of chloride ion are described in Table 5.

5. Conclusions

The conclusions of this study on evaluation technique for chloride penetration in high performance concrete using neural network algorithm and micro pore structures are as follows.

1) The evaluation technique for chloride penetration behavior with time-dependent diffusion coefficient obtained from neural network algorithm and micro models considering behaviors in early-age concrete is developed. Through the comparison of experimental data and numerical simulation results, the developed technique is shown to have rational applicability to different mixture designs of HPC.
2) It is shown that diffusion coefficients can be estimated successfully through neural network algorithm having 8 neurons, which are 7 components in mixture design and duration time in submerged condition. For 120 data-set of diffusion coefficients, average of difference between estimated results from neural network and from experimental data is evaluated to be 7.5%.
3) By utilizing more extensive and quantitative data-set considering mineral admixtures, time duration, and a large number of test specimens, this proposed technique on neural network algorithm can be more effective for evaluation of chloride penetration.

Acknowledgment

The authors acknowledge the financial support by a project on Standardization of Construction Specifications and Design Criteria based on Performance and support by Concrete Corea Center, Korea and data by Samsung Construction LTD., Korea.

References

[1] M. Nagesh, B. Bishwajit, Modeling of chloride diffusion in concrete and determination of diffusion coefficients, ACI Mater. J. 92 (1998) 113–120.
[2] L. Tang, Chloride Transport in Concrete, Division of Building Materials, Chalmers University of Technology, Sweden, 1996 Publication P-96:6.
[3] L. Tang, L.O. Nilsson, Chloride binding capacity and binding isotherms of OPC paste and mortar, Cem. Concr. Res. 23 (1993) 347–353.
[4] K. Maekawa, T. Ishida, T. Kishi, Multi-scale modeling of concrete performance, J. Adv. Concr. Technol. 1 (2003) 91–126.
[5] H.-W. Song, S.-J. Back, C.-H. Lee, S.-J. Kwon, Service life prediction of concrete structures under marine environment considering coupled deterioration, J. Restor. Build. Monum. 12 (4) (2006) 265–284.
[6] H.-W. Song, J.-C. Jang, V. Saraswathy, K.-J. Byun, An estimation of the diffusivity of silica fume concrete, Build. Environ. 42 (3) (2007) 1358–1367.
[7] T. Ishida, M. Maekawa, Modeling of durability performance of cementitious materials and structures based on thermo-hygro physics, Rilem Proceedings PRO 29: Life Prediction and Aging Management of Concrete Structures, 2003, pp. 39–49.
[8] Korea Concrete Institute, Concrete Standard Specification — Durability Part, 2004.
[9] JSCE-Concrete committee, Standard Specification for Concrete Structures, 2002.

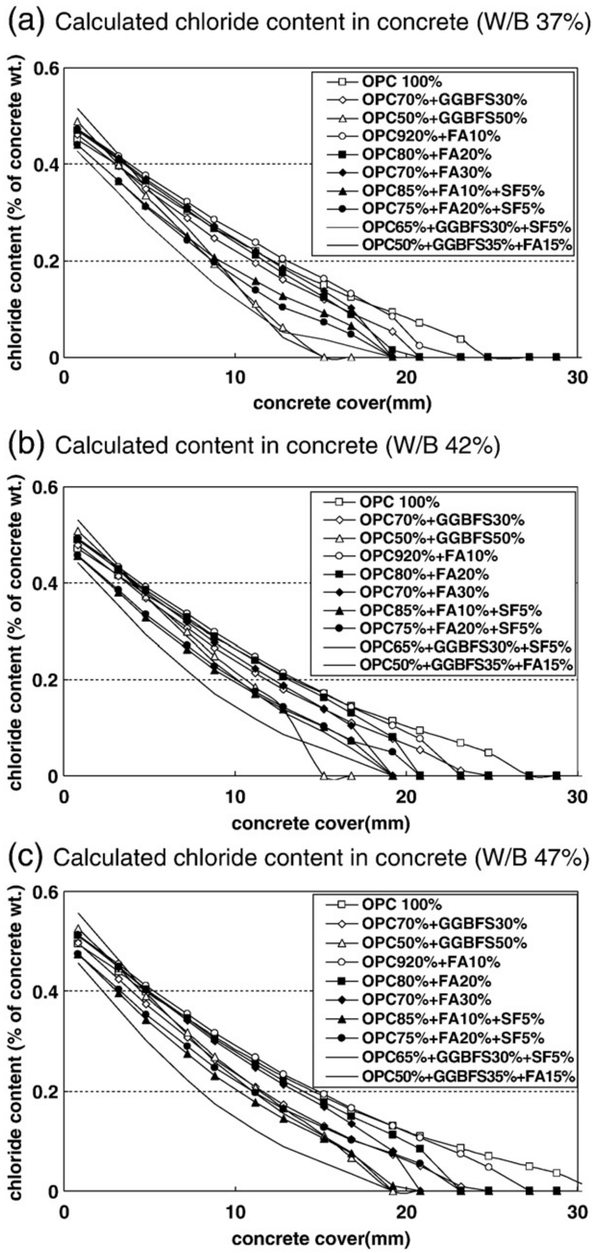

Fig. 9. Calculated chloride content with same water to binder ratio.

Table 7
Mix proportions [34] and estimated results of chloride diffusion coefficient.

Water to binder (%)	Cement (kg/m^3)	Fly ash (kg/m^3)	Water (kg/m^3)	Sand (kg/m^3)	Gravel (kg/m^3)	Obtained from this study	
						Diffusion coefficient ($\times 10^{-11}$ m^2/s)	m
38	449	–	171	616	1050	0.48234	0.20
38	359	90	171	616	1050	0.46973	0.40

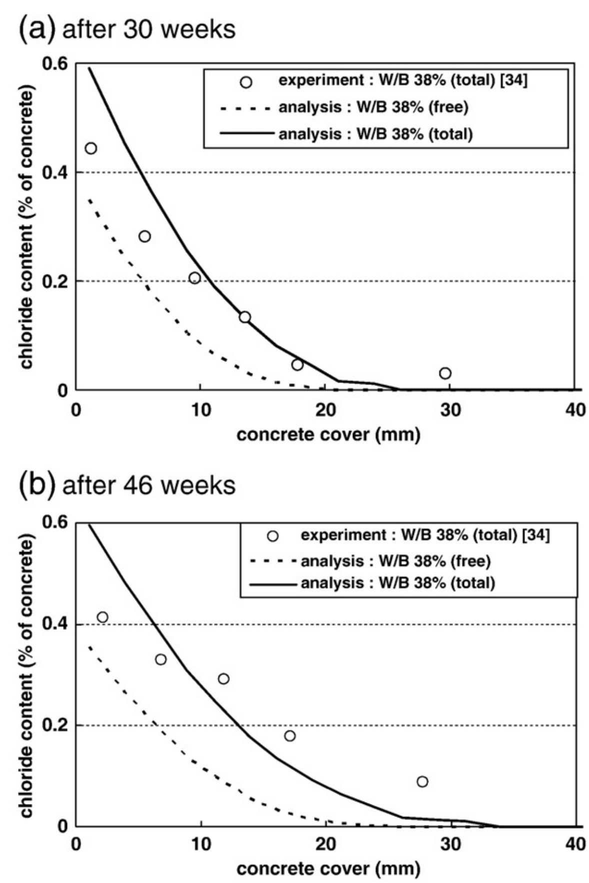

Fig. 10. Comparison of experimental and numerical results (OPC 100%).

[10] M.D.A. Thomas, E.C. Bentz, Computer Program for Predicting the Service Life and Life-cycle Costs of Reinforced Concrete Exposed to Chlorides, SFA, 2002 Life365 Manual.
[11] I.-C. Yeh, Modeling slump flow of concrete using second-order regressions and artificial neural networks, Cem. Concr. Compos. 29 (2007) 474–480.
[12] W.P.S. Dias, S.P. Pooliyadda, Neural networks for predicting properties of concretes with admixtures, Constr. Build. Mater. 15 (7) (2001) 371–379.
[13] J. Bai, S. Wild, J.A. Ware, B.B. Sabir, Using neural networks to predict workability of concrete incorporating metakaolin and fly ash, Adv. Eng. Softw. 34 (11–12) (2003) 663–669.
[14] J.-Z. Wang, H.-G. Ni, J.-Y. He, The application of automatic acquisition of knowledge to mix design of concrete, Cem. Concr. Res. 29 (1999) 1875–1880.
[15] J.A. Stegemann, N.R. Buenfeld, Prediction of unconfined compressive strength of cement paste with pure metal compound additions, Cem. Concr. Res. 32 (2002) 903–913.
[16] I.-C. Yeh, Modeling of strength of high-performance concrete using artificial neural networks, Cem. Concr. Res. 28 (1998) 1797–1808.
[17] K.B. Park, T. Noguchi, J. Plawsky, Modeling of hydration reactions using neural networks to predict the average properties of cement paste, Cem. Concr. Res. 35 (2005) 1676–1984.
[18] K. Maekawa, R. Chaube, T. Kishi, Modeling of Concrete Performance: Hydration, Microstructure Formation and Mass Transport, Routledge, London, 1999.
[19] W. McCulloch, W. Pitt, A logical calculus of the ideas immanent, Bull. Math. Biophys. 5 (1943) 115–133.
[20] H. Demuth, M. Beale, Neural Network Toolbox: User's Guide, The MathWorks, Inc., 1997.
[21] ASTM C 1202, Annual Book of ASTM Standards, 1997 v.04.02.
[22] L. Tang, Electrically accelerated methods for determining chloride diffusivity in concrete-current development, Mag. Concr. Res. 48 (1996) 173–179.
[23] L. Tang, L.O. Nilsson, Rapid determination of the chloride diffusivity in concrete by applying an electrical field, ACI Mater. J. 89 (1992) 49–53.
[24] N. Otsuki, S. Nagataki, K. Nakashita, Evaluation of $AgNO_3$ solution spray method for measurement of chloride penetration into hardened cementitious matrix materials, ACI Mater. J. 89 (1992) 587–592.
[25] L. Tang, G. Joost, On the mathematics of time-dependent apparent chloride diffusion coefficient in concrete, Cem. Concr. Res. 37 (2007) 589–595.
[26] E. Poulsen, On a model of chloride ingress into concrete, Nordic Miniseminar-Chloride Transport, Department of Building Materials, Chalmers University of Technology, Gothenburg, 1993, pp. 1–12.
[27] A. Neville, Chloride attack of reinforced concrete : an overview, Mat. Struct. 28 (176) (1995) 63–70.
[28] K. Tuutti, Corrosion of Steel in Concrete, Swedish Cement and Concrete Research Institute(CBI), Stockholm, Sweden, 1982 CBI Report no. 4-82.
[29] H.-W. Song, S.-J. Kwon, K.J. Byun, C.K. Park, Predicting carbonation in early-aged concrete, Cem. Concr. Res. 36 (2006) 979–989.
[30] H.-W. Song, S.-J. Kwon, Permeability characteristics of carbonated concrete considering capillary pore structure, Cem. Concr. Res. 37 (2007) 909–915.
[31] T. I shida, R.P. Chaube, K. Maekawa, Modeling of pore content in concrete under generic drying wetting conditions, Concr. Libr. JSCE 18 (1996) 113–118.

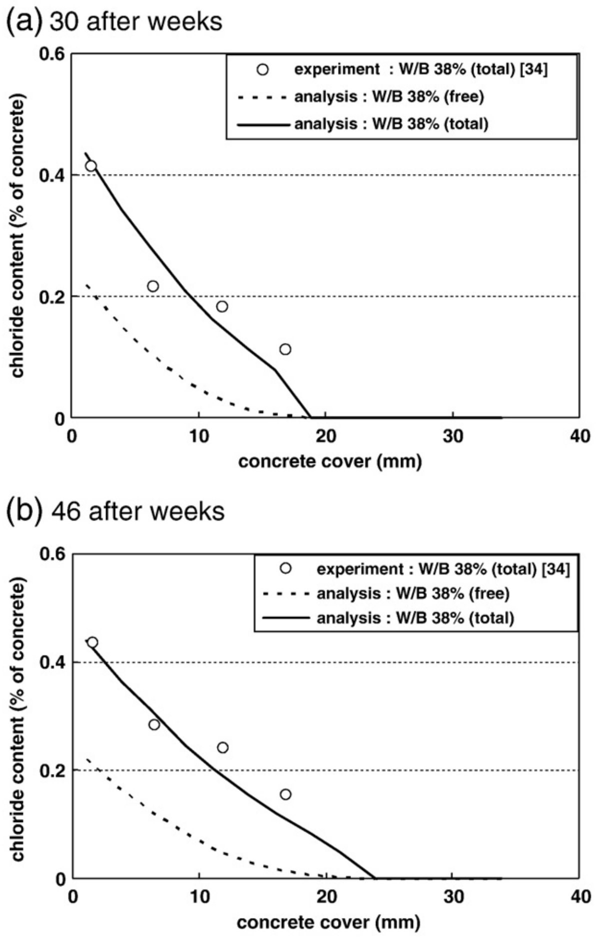

Fig. 11. Comparison of experimental and numerical results (OPC 80% + FA 20%).

[32] T. Ishida, K. Maekawa, T. Kishi, Enhanced modeling of moisture equilibrium and transport in cementitious materials under arbitrary temperature and relative humidity history, Cem. Concr. Res. 37 (2007) 565–578.
[33] AASHTO, Standard method of test for sampling and testing for chloride ion in concrete and concrete raw materials. *AASHTO T260-97*: American Association of State Highway and Transportation Officials, Washington, D.C., 898–904.
[34] S.Y. Jang, Modeling of chloride transport and carbonation in concrete and prediction of service life of concrete structures considering corrosion of steel reinforcement, Ph. D. Dissertation, Dept. of Civil Engineering, Seoul National University, Korea, 2003.